

Rock-Flow Cell Parameters Evaluation Using Ultrasound Doppler Velocimetry

Stakowian, Andre, L.¹, Dextre, Gino N. D.⁵, Botton, Luís F.¹, Dos Santos, Eduardo, N.¹, Coutinho, Fabio, R.², Ofuchi, César, Y.¹, Da Silva, M, J.³, De Cesare, G.⁴, Morales, R, E, M.⁵, Mariette, O.⁶

¹ Graduate School of Electrical Engineering and Computer Science (CPGEI), Federal University of Technology - Paraná (UTFPR), Av. 7 de Setembro 3165, Curitiba, 80230-901, Parana, Brazil.

² Dep. of Electronics Engineering, Federal Univ. of Technology - Paraná (UTFPR), R. Cristo Rei 19, Vila Becker, Toledo, Parana, 85902-490, Brazil.

³ Institute of Measurement Technology, Johannes Kepler University Linz, Altenberger Str. 69, 4040, Linz, Austria.

⁴ Platform of Hydraulic Constructions (PL-LCH), École Polytechnique Fédérale de Lausanne (EPFL), CH1015 Lausanne, Switzerland.

⁵ Mechanical & Materials Engineering Postgraduate Program (PPGEM), Federal University of Technology - Paraná (UTFPR), Av. 7 de Setembro 3165, 80230-901, Curitiba, Parana, Brazil.

⁶ Met-Flow S.A, Chemin Auguste-Pidou 8, 1007 Lausanne, Switzerland.

This work presents a study of two-phase flow generated inside a rock-flow cell setup. It is characterized by a pipe section filled with fluid (oil in our studies) that is put into oscillation around its mass centre by an electric motor. This type of apparatus has been used by some research groups worldwide to mimic the flowing conditions of complex pipe multiphase flows but with the advantage of being compact in size. In this work, a rock flow cell was used to characterize stratified-wavy and slug flow regimes to investigate the phenomenological dynamics and behaviour around the liquid interface. The experimental procedure cases covered two total cell liquid loadings (30% and 75%), and the setup configuration was kept the same in terms of angular frequency oscillation (100 rpm) and oscillation angle amplitude (19°). Ultrasound Doppler Velocimetry (UDV) was used to monitor and assess the flow field velocity behaviour and distribution inside a rocking pipe, obtained through the EAM (Extended Auto-Correlation Method) velocity estimator algorithm. From the resulting velocity profile, we estimated the shear rate parameter. Furthermore, we could identify the air-oil phase interface position using the echo amplitude information. The UDV technique applied to rock-flow cell has a great potential to generate detailed flow information, which in turn can be used, for example, to validate Computational Fluid Dynamics (CFD) numerical simulations.

Keywords: Rock-Flow Cell, Doppler Velocimetry, Multi-Phase Flow, Velocity Profile.

1. Introduction

As the interest in a better understanding of flows' behaviour and characterization has grown through the last decades, various methods and technologies have emerged to shed more light on the fluid dynamics research field. Amongst some of the approaches to working with the fluid dynamics field, we can mention optical methods such as Particle Image Velocimetry (PIV), which require both the fluid and its casing to be transparent and has high implementation and computational costs. Electrical impedance and conductance probes, which are invasive options prone to lead to flow disturbances. On the other hand, ultrasound-based methods, such as Ultrasound Doppler Velocimetry (UDV), have the desirable advantages of being non-invasive, non-intrusive, capable of working with opaque fluids, and ease of installation and operation [1]. The UDV method also encounters applications in various industry and research fields such as nuclear plants, food engineering, chemical plants, oil and gas exploitation and transportation [2], [3].

The ideal scenario for studying the flow behaviour would be having access to real plants and installations, which is only sometimes possible and would be costly. Thus, alternatives have to be found to promote the studies. Such

options are flow loops, which can be built in different configurations, trying to resemble the real plants and installations, enabling the assessment of characteristics of the phenomena in more detail. Another option is the rock-flow cells, which have the advantage of being compact in size and able to produce complex multiphase flows, using fewer resources as, for example, the reduced volume of the liquid phase. The main applications of rock-flow cells are in the flow assurance field, where hydrate formation and deposition are studied [4], [5], and also the assessment of hydrate mitigation methods [6], [7].

In this work, we first present the stratified-wavy flow assessment, a more straightforward flow pattern through which we could understand the experimental process and signal processing. Then, the slug flow pattern is addressed with a higher level of liquid loading. This type of flow is commonly found in multiphase flows, receiving particular attention due to their presence in various applications, particularly in the oil and gas industry. This specific flow pattern poses a significant challenge in fluid transportation due to problems associated with pipeline corrosion caused by the erosion of anticorrosive materials. Additionally, the mixing region of slugs enhances hydrate formation, one of the significant concerns in flow assurance. In such scenarios, the presence of bubbles originates from the

detachment of the gas phase at the rear of the long bubble. This detachment is caused by an imbalance of forces, primarily resulting from excessive shear near the fluid interface. This paper proposes the use of a new approach for estimating the shear rate using the US method in the rock-flow cell configuration.

The shear rate parameter may suffer from multidimensional velocity vectors, however, in this work we are primarily interested in the shear force in the vertical ultrasound beam plane. In this scenario, the shear rate is estimated from the field velocity (in the flow direction), calculated through the following relation: $\varepsilon = \partial u / \partial y$; where ε is the shear rate (s^{-1}) to be analyzed, u (m/s) the particle velocity in x direction (flow direction), y (m) position of pipe section.

2. Experimental Set-Up and Methodology

The experimental apparatus developed for the experiments and results presented in this work is named Rock-Flow Cell. It consists of a 1200 mm long acrylic pipe with a 50 mm inner diameter, mounted on an aluminum frame with an oscillating pivot (Figure 1). One engine performed the RFC oscillating movement through a connecting rod and crank system. An accelerometer located at one edge of the pipe measured the oscillation frequency and oscillation amplitude range, which were kept at 100 rpm and 19° , respectively, throughout the whole experimental set. Images were captured through a high-definition camera (Logitech c920) and processed in the MatLab® 2019b release.

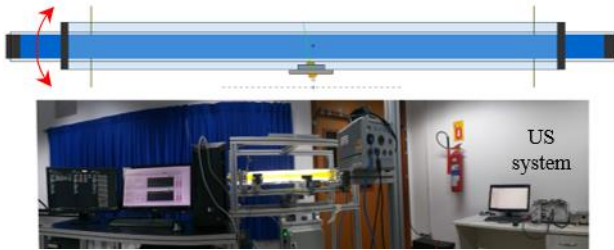


Figure 1: Rock-Flow Cell schematic description.

The test fluid is a mineral oil, which density is $843.32 \text{ (kg/m}^3\text{)}$, its viscosity is 0.0687 (kg/ms) , and its superficial tension is 0.031 (N/m) . We worked with two distinct total cell liquid loadings (30% and 75%, concerning the total cell volume) as our experimental cases; the amount of oil, in volume, corresponding to each liquid loading, was weighted, mixed with yellow dye to identify the air-oil interface better, and poured inside the pipe. An acrylic box filled with water was disposed around the pipe to reduce the light refraction effect and, thus, the distortion of the image captured by the camera. A frequency inverter was applied to regulate the oscillation speed (100 rpm).

The instrumentation of the rock-flow cell was made through a 4 MHz ultrasonic transducer, positioned beneath the pipe, aligned with its axis, and at 10° to the pipe's cross-sectional plane. The data set was acquired using the National Instruments-based PXIe-1078 chassis with a

PXIe-7966R FPGA module. The entire signal post-processing has been done offline in the MatLab® 2019b release. Polyethylene seeding particles of 937 kg/m^3 , with a mean diameter of around $250 \text{ }\mu\text{m}$, were added and mixed with the oil phase. These particles played the role of tracers for the Ultrasonic Doppler technique.

The experimental approach, briefly described, was as follows: initially, we positioned the pipe section perfectly horizontally, with the aid of an electronic angle meter; then we started the data acquisition system; after about 2.5 seconds, we started the motion system. We intentionally did this process to capture a portion of the flat, steady state, part of the liquid phase, which enabled us to confirm the liquid loading through the liquid height obtained from the ultrasound backscattered signal. Finally, the offline post-processing part encompasses the air-oil phase interface identification through the amplitude threshold technique from the raw, backscattered signal [8] and the velocity map obtained through the Extended Auto-Correlation Method (EAM) [9].

3. Results and Discussions

In this section, we provide a qualitative and quantitative discussion about the outcomes of our experiments. Figure 2 displays the phase interface estimated and the velocity map for the 30% of liquid loading. Given this level of cell filling, we have the stratified-wavy flow pattern developed, characterized by the undulatory behaviour of the liquid phase that does not touch the upper part of the pipe. In the first nearly 2.5 seconds the cell was kept in its steady state, and then the system was put into oscillation. In this figure, we can also see two well-defined, alternating equivalent behaviour regions, governed by the direction of oscillation of the rock-flow cell. R1 and R2 represent the clock-wise sense of motion of the rock-flow cell, where the flow moves away from the transducer, and R3 and R4 being the opposite.

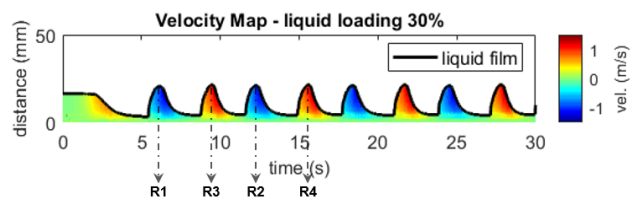


Figure 2: Stratified-wavy flow pattern obtained with 30% of total liquid loading.

Additionally, from the velocity map (Figure 2) we can observe that the magnitude of velocity field distribution is higher on the back of the wave structure. In a similar manner, we compared the mean velocity profiles for the corresponding lines R3 and R4, as shown in Figure 4.

Figure 3 depicts the instantaneous velocity profiles along lines R1 and R2, exhibiting an equivalent behavior between them, and good agreement in terms of shape and magnitude, also reproducing the no-slip condition at the wall surface. We noticed that an oscillation frequency of 100 rpm results in a max velocity of about 0.75 m/s in both directions.

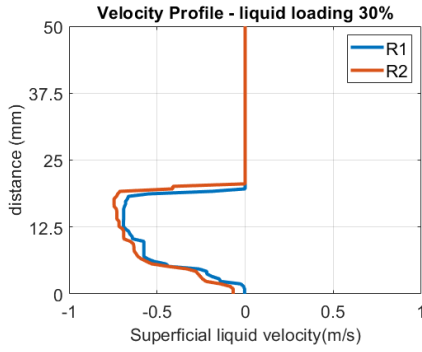


Figure 3: Comparison of velocity profiles for the equivalent behaviour regions R1 and R2.

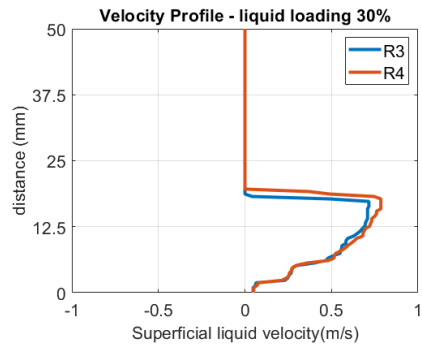


Figure 4: Comparison of velocity profiles for the equivalent behaviour regions R3 and R4.

From the velocity profiles (Figure 3 and Figure 4), we also calculated the shear rate parameter, shown in the Figure 5 and Figure 6.

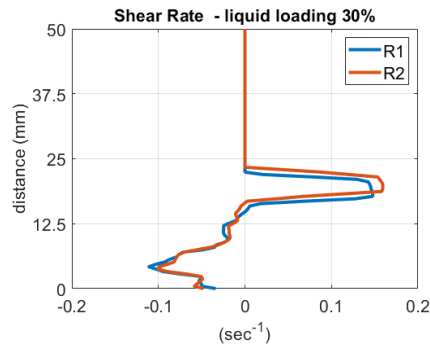


Figure 5: Comparison of the shear rate parameter for the equivalent behaviour regions R1 and R2.

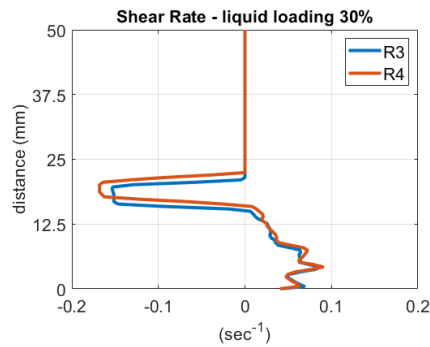


Figure 6: Comparison of the shear rate parameter for the equivalent behaviour regions R3 and R4.

As expected, both the oil-air interface and the pipe wall experience the effects of liquid shear stress. This stress is slightly more pronounced at the air-oil phase interface due to the counter-flow pattern, wherein the liquid flows in the opposite direction to the gas. In this configuration, the region near the interface of the fluid layers undergoes a relative movement.

Figure 7 illustrates the velocity map for the liquid loading of 75%. At this level of cell filling, we have the slug flow pattern developed, characterized by alternating gas bubbles and slug body structures. As we could expect, the slug flow is a more complex flow pattern compared to the stratified-wavy, resulting in a diversified range of outcomes.

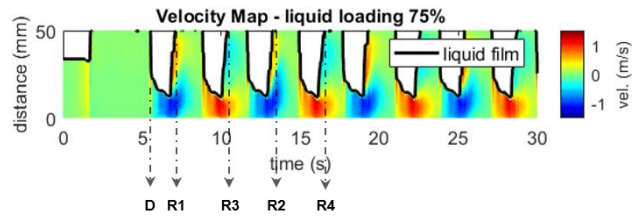


Figure 7: Slug flow pattern obtained with 75% of total liquid loading.

In the flow map (Figure 7), one can notice that we have two distinct field velocity distributions at each slug unit that repeat themselves throughout the equivalent behaviour regions. In Figure 7, the region labeled as 'D' indicates that the leading edge of the slug bubbles, often referred to as the bubble nose, carries a certain amount of oil mass with it due to viscous effects, and this phenomenon occurs in both directions.

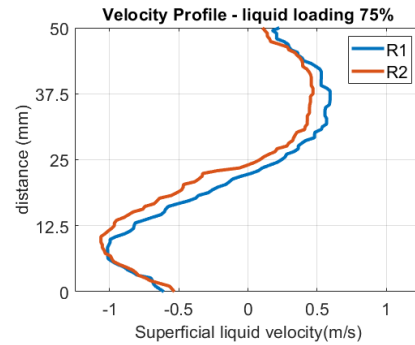


Figure 8: Comparison of velocity profiles for the equivalent behaviour regions R1 and R2.

Figure 8 and Figure 9 highlight the velocity profile lines plotted at the rear part of the slug bubble, where it is possible to see the changes in velocity direction between liquid film and slug body. This is due to the high turbulence and mixing factor at the bubble tail.

As the proposal is to estimate the shear rate at the end of the bubble, the pair of positions R1-R2 and R3-R4 were selected. The behaviour in both cases follows the aforementioned results, demonstrating acceptable repeatability.

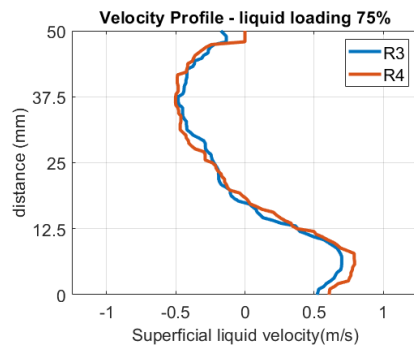


Figure 9: Comparison of velocity profiles for the equivalent behaviour regions R3 and R4.

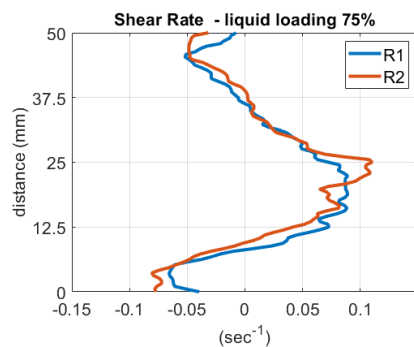


Figure 10: Comparison of the shear rate parameter for the equivalent behaviour regions R1 and R2.

It is interesting to note that the shear rate, at the positions selected, reaches a peak in magnitude at the inflection point portion of the flow, where the velocity fields change direction, which occurs approximately at 25 mm for regions R1 and R2 (Figure 10), and at 12.5 mm for regions R3 and R4 (Figure 11), respectively.

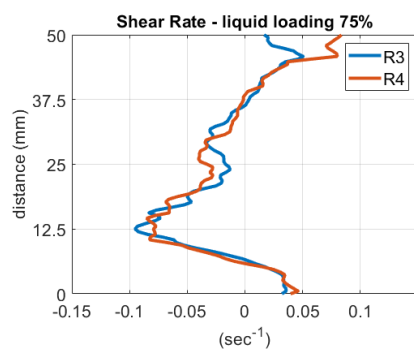


Figure 11: Comparison of the shear rate parameter for the equivalent behaviour regions R3 and R4.

4. Summary

In this work, we presented a novel and insightful application for the Ultrasonic Doppler Velocimetry technique. We could instrument a Rock-Flow Cell, an innovative laboratory-scaled flow generator, and analyze two different flow patterns.

From the results, we found that the UDV technique was able to successfully characterize the stratified-wavy and slug flow patterns in terms of phase interface identification and velocity field distribution. Through further analysis of

the velocity profiles and velocity maps we could qualitatively and quantitatively describe the velocity behavior in different structures for both flow patterns. Thus, some overall and conclude remarks can be drawn:

- For the stratified-wave flow, the velocity profiles are similar in shape and magnitude, in both directions, as expected, and the velocity field distribution magnitude is higher at the rear part of the wave structure, which we believe is due to the increasing flow momentum. The shear rate was found to be slightly greater at the phase interface.
- With the slug flow pattern the observations were that we have two well defined velocity fields on each slug structure. One is at the liquid film portion, and the other is at the slug bubble tail, which is also a highly turbulent and mixing region, and the velocity fields develop in opposite directions. This behaviour is also highlighted and confirmed with the velocity profiles. The highest level of shear rate occurs at the intersection of the two velocity regions of the slug unit

Acknowledgements

The authors would like to acknowledge the support from the following agencies: ANP, FINEP and MCT, through the Human Resources Program of ANP for the oil and gas sector. Also, to PETROBRAS for the rock-flow cell project funding and CNPq.

References

- [1] Y. Takeda, Ultrasonic Doppler Velocity Profiler for Fluid Flow, vol. 101. 2012.
- [2] C. Tan, *et al.*, "Ultrasonic Doppler Technique for Application to Multiphase Flows: A Review," Int. J. Multiph. Flow, vol. 144, no. August, p. 103811, 2021, doi: 10.1016/j.ijmultiphaseflow.2021.103811.
- [3] C. Y. Ofuchi, *et al.*, "Evaluation of an extended autocorrelation phase estimator for ultrasonic velocity profiles using nondestructive testing systems," Sensors (Switzerland), vol. 16, no. 8, 2016, doi: 10.3390/s16081250.
- [4] X. Liu, *et al.*, "Experimental investigation on the process of hydrate deposition using a rock-flow cell," Fuel, vol. 305, no. August, p. 121607, 2021, doi: 10.1016/j.fuel.2021.121607.
- [5] E. O. Straume, *et al.*, "Experimental study of the formation and deposition of gas hydrates in non-emulsifying oil and condensate systems," Chem. Eng. Sci., vol. 155, pp. 111–126, 2016, doi: 10.1016/j.ces.2016.07.046.
- [6] Y. Liu, *et al.*, "Experimental study on the gas hydrates blockage and evaluation of kinetic inhibitors using a fully visual rocking cell," J. Nat. Gas Sci. Eng., vol. 96, no. October, p. 104331, 2021, doi: 10.1016/j.jngse.2021.104331.
- [7] C. Yu, *et al.*, "Screening Hydrate Antiagglomerants for an Oil-Gas-Water System from Various Commercial Chemicals Using Rocking Cells," Energy and Fuels, vol. 36, no. 18, pp. 10685–10701, 2022, doi: 10.1021/acs.energyfuels.2c01285.
- [8] Y. Murai, *et al.*, "Ultrasonic detection of moving interfaces in gas – liquid two-phase flow," Flow Meas. Instrum., vol. 21, no. 3, pp. 356–366, 2010, doi: 10.1016/j.flowmeasinst.2010.03.007.
- [9] C. Y. Ofuchi, *et al.*, "Extended Autocorrelation Velocity Estimator Applied to Fluid Engineering," in ISUD, 2014, pp. 109–112.